# Ab Initio Study of the Ne($^1$S)−CN($^2\Sigma^+$) van der Waals Complex

**Imrich Vrábel,*,† Vladimír Lukeš,‡ Viliam Laurinc,‡ and Stanislav Biskupič†**

*Departments of Physical Chemistry and Chemical Physics, Slovak University of Technology, Radlinského 9, SK-81237 Bratislava, Slovak Republic*

*Received: July 20, 1999; In Final Form: October 27, 1999*

The Ne($^1$S)−CN($^2\Sigma^+$) van der Waals complex, described by Jacobi coordinates ($R$, $\Theta$), was studied using the supermolecular and perturbation UHF as well as RHF ab initio treatments with the inclusion of correlation energy. The computed potential energy surface at the restricted MP2 level of the theory reveals a single minimum, located near the T-shaped configuration at $\Theta = 110°$, $R = 3.7$ Å, and its well depth amounts to $-145.9\ \mu E_h$. When compared with the RMP2 potential, the UMP2 surface is more repulsive in the region of the minimum and the double-well character of the angular-dependent potential curves appears about $R \approx 3.7$ Å. The position of the minimum is nearer to the C end, at $R \approx 3.7$ Å and $\Theta = 50°$. The influence of the selected geometry variations on the fundamental energy components, obtained from intermolecular perturbation theory, was also investigated. The separation of the interaction energy shows that the shape and location of these minima are primarily determined by the anisotropy of the exchange-penetration and dispersion components.

## Introduction

The knowledge of the inter- and intramolecular potential-energy surfaces (PES) is essential for the understanding of many physical, chemical, and biological processes and properties of molecules and clusters. The main experimental sources of information about PES of complexes are the high-resolution spectroscopic studies[1−4] and the scattering experiments.[5−9] In contrast to weakly bonded neutral clusters containing closed-shell molecules, such experimental data are rare for neutral open-shell complexes.[10−16] However, the forces acting between a pair of open-shell and closed-shell atoms or molecules are interesting from the chemical point of view, as they often exhibit high reactivities and appear as transient intermediates in the reactions.[17] Furthermore, as shown by Heaven,[12] these complexes offer a unique opportunity to bridge the gap between a weak van der Waals (vdW) interaction and an incipient chemical bond. In addition, since the seminal work of Lin and Heaven,[18] the dynamics of the rare gas open-shell molecules has served as an important model problem for understanding nonadiabatic predissociation processes.

The CN−rare gas (He, Ne, Ar) system has been one of the prototypes for the study of a collision-induced electronic energy transfer. This process is facilitated by a series of near resonances between the vibrational manifolds of the ground (X $^2\Sigma^+$) and first two excited states (A $^2\Pi$, B $^2\Sigma^+$) of the cyano radical. Quenching of the electronically excited CN was observed in CN-doped Ne matrixes[19] and in the gas phase.[20] Dagdigian and co-workers[6−9] have carried out the detailed state-to-state experiments. They investigated the energy transfer from A $^2\Pi$ to X $^2\Sigma^+$ induced by collisions with Ar using optical−optical double resonance. Halpern and Huang[21] also examined the collisional fluorescence quenching of A $^2\Pi \rightarrow$ X $^2\Sigma^+$ transfer for the collision partners He, Ne, and Ar. More recently, Heaven's group[22] has observed a nonadiabatic predissociation process between A $^2\Pi_{1/2}$ and A $^2\Pi_{3/2}$ spin−orbit states.

The general theoretical description of these processes arises from Alexander and Corey.[23] Subsequently, Werner and co-workers[24] published the first ab initio determination of diabatic PESs for the computationally less time-consuming He−CN system. This work was followed later by quantum scattering calculations[25] and the theoretical predictions for He−CN were compared with the experiments on the Ar−CN system. Recently, Yang and Alexander[26] have reported a similar multireference configuration interaction (MR-CI) study for the Ne−CN system. In their publication the electronically adiabatic and diabatic ab initio PESs were determined for the interaction of Ne with the ground, X $^2\Sigma^+$, and first excited, A $^2\Pi$, electronic states of the CN radical.

From the previous brief survey it is evident that the theoretical description of open-shell vdW complexes has been dominated by the nonperturbative supermolecular methods such as the coupled electron pair approximation[27,28] or MR-CI,[29] because they enabled calculations of excited states of different symmetries and multiplicities. Furthermore, they can efficiently deal with the avoided crossing problem and with the states that cannot be easily described by single-determinant wave functions. However, these methods have also some natural limitations. The truncated CI methods are not size-consistent and do not permit a direct decomposition of the interaction energy into physically meaningful terms. In addition, the MR-CI calculations usually do not take into account all triple and quadruple excitations that are necessary to describe vdW complexes accurately.[30] Finally, for the multideterminant calculations it is not easy to ensure the unambiguous correction to the basis set superposition error (BSSE).[31] Nevertheless, these limitations can be bypassed by the supermolecular unrestricted Møller−Plesset perturbation theory (UMPPT).[32−35] Although this method is less versatile than MR-CI in treating excited states, it offers an important alternative and a supplemental approach, if the perturbation expansion is reasonably well converged and the spin contamination is small. The efficiency of the UMPPT accompanied by the intermolecular perturbation theory (I-PT) has been recently

---

† Department of Physical Chemistry.

‡ Department of Chemical Physics.

10.1021/jp992485n CCC: $19.00

established for several open-shell cases, in particular He−O$_2$ (X $^3\Sigma_g^-$),[35] Ar−NH ($^3\Sigma^-$),[36] He−CH (X $^2\Pi$),[37] and He−Cl ($^2P$).[38]

Unfortunately, in contrast to the above-mentioned complexes, the spin contamination causes a serious problem for Ne−CN($^2\Sigma^+$). Therefore, the application of the unrestricted perturbation theory to this system is questionable. In this case, the employment of the perturbation theory with the RHF reference wave function, which is well-defined with respect to the spin operator $\hat{S}^2$, offers an alternative solution.[39−41] Although, in general, the Hamiltonian matrix elements provided by the RHF solutions for the open-shell monomers are not invariant with respect to the arbitrary orthogonalization procedures,[42] the computational requirements on the hardware and time capacities for this approach are at least 4 times lower in comparison with the UHF case due to the identity of the $\alpha$ and $\beta$ wave functions.

The main goal of this paper is to reinvestigate the selected portions of the PES for the Ne−CN($^2\Sigma^+$) complex and to compare the ability of the single-determinant RHF and UHF reference wave functions for this numerically troublesome system. In this context, the anisotropy of the interaction energy in terms of the basic components will be presented in a manner similar to the closed-shell complexes based on the I-PT applicable to the open-shell systems. It might be helpful to understand the physical background of the stability, which can be relevant for the experimental measurements of the above-mentioned weakly bonded molecule. Finally, the importance of the zero-point energy corrections will be shortly discussed.

## Theoretical Approach

The ab initio methods used for the calculations of interaction energies can be classified as supermolecular, perturbative, and hybrid ones.[31] The supermolecular treatment defines the interaction energy corrections as a difference between the value of the total energy of the dimer (AB) and the sum of the subsystem energies (A, B) for each order of the perturbation theory separately

$$\Delta E^{(n)} = E_{AB}^{(n)} - E_{A}^{(n)} - E_{B}^{(n)} \qquad n = \text{HF}, 2, 3, 4, ... \quad (1)$$

The intermolecular perturbation theory (I-PT) calculates the interaction energy directly as a sum of the electrostatic ($E_{\text{es}}$), exchange-penetration ($E_{\text{exch}}$), induction ($E_{\text{ind}}$), dispersion ($E_{\text{disp}}$), etc. energies. Applying the standard Rayleigh−Schrödinger perturbation theory, one can derive the many-body expansion of the interaction energy corrections

$$E_{\text{int}} = \sum_{n=0}^{\infty}\sum_{i=0}^{\infty}\sum_{j=0}^{\infty} E_{\text{es}}^{(nij)} + \sum_{n=0}^{\infty}\sum_{i=0}^{\infty}\sum_{j=0}^{\infty} E_{\text{exch}}^{(nij)} + \sum_{n=2}^{\infty}\sum_{i=0}^{\infty}\sum_{j=0}^{\infty} E_{\text{ind}}^{(nij)} + \sum_{n=2}^{\infty}\sum_{i=0}^{\infty}\sum_{j=0}^{\infty} E_{\text{disp}}^{(nij)} + ... \quad (2)$$

where $n$ represents the order of the interaction perturbation. The symbols $i$ and $j$ stand for the order of the correlation operator of the systems A and B, respectively.[43] The general problem of expanding the individual terms in eq 2 through one- and two-electron integrals can be elegantly resolved via the diagrammatic representation of the perturbation expansion. The exchange effects may be specified in different ways.[43−45]

The supermolecular interaction energies can be successfully separated using the perturbation calculation of the interaction energy components. The SCF interaction energy can be decomposed as follows

$$\Delta E^{\text{HF}} = \Delta E^{\text{HL}} + \Delta E_{\text{def}}^{\text{HF}} \quad (3)$$

where $\Delta E^{\text{HL}}$ is the Heitler−London (HL) energy and $\Delta E_{\text{def}}^{\text{HF}}$ is the so-called HF deformation contribution.[31] $\Delta E_{\text{def}}^{\text{HL}}$ is defined by Löwdin[46] as

$$\Delta E^{\text{HL}} = \frac{\langle \hat{A}\Psi_A\Psi_B|\hat{H}_{AB}|\hat{A}\Psi_A\Psi_B\rangle}{\langle \hat{A}\Psi_A\Psi_B|\hat{A}\Psi_A\Psi_B\rangle} - E_A^{\text{HF}} - E_B^{\text{HF}} \quad (4)$$

where $\hat{A}$ is the dimer antisymmetrization operator and $\Psi_A$ and $\Psi_B$ are the HF wave functions of the monomers. The HF energies of the A and B system are denoted by $E_A^{\text{HF}}$ and $E_B^{\text{HF}}$, respectively. According to the I-PT theory defined in the orthogonalized basis sets,[44,45] $\Delta E^{\text{HL}}$ may be further divided into the HF electrostatic $E_{\text{es}}^{(100)}$ and HL exchange-penetration $E_{\text{exch}}^{\text{HL}}$ components

$$E_{\text{es}}^{(100)} = \langle \Psi_A\Psi_B|\hat{V}_{AB}|\Psi_A\Psi_B\rangle \quad (5)$$

$$E_{\text{exch}}^{\text{HL}} = \Delta E^{\text{HF}} - E_{\text{es}}^{(100)} \quad (6)$$

$\Delta E_{\text{def}}^{\text{HF}}$ originates from the mutual electric polarization effects and, in contrast to the perturbation term $E_{\text{ind}}^{(200)}$ (HF second-order induction energy), it may be viewed mainly as the quantum induction including the corresponding repulsive exchange-penetration effects.[31] The contribution $E_{\text{ind}}^{(200)}$ is evaluated in the framework of the uncoupled HF level of theory.[47] A more accurate approach requires additional inclusion of the so-called response or orbital-relaxation effects.[48,49]

Similarly to the closed-shell cases, the second-order correlation interaction energy of the open-shell systems can be formally partitioned as

$$\Delta E^{(2)} = E_{\text{disp}}^{(200)} + \Delta E_{\text{exch}}^{(2)} + \Delta E_{\text{other}}^{(2)} \quad (7)$$

where $E_{\text{disp}}^{(200)}$ represents the second-order HF dispersion energy. $\Delta E_{\text{exch}}^{(2)}$ involves the second-order exchange-correlation energies. The subscript "other" denotes the electrostatic-correlation, deformation-correlation corrections and the response effects as well as the "exchange-deformation" terms.[31,43] The evaluation of the higher than second-order interaction energy contributions is also possible. However, their complete physical interpretation is, in general, not straightforward.

## Calculation Details

All I-PT calculations were performed by our program codes interfaced to the Gaussian 94 program package.[50] The supermolecular BSSE was determined via the standard counterpoise method of Boys and Bernardi.[51] The presented single-reference RHF and UHF interaction energy terms were developed using the dimer-centered basis sets (DCBS)[31] of the constituent monomers, and the first term in eq 4 was obtained using the standard Gram−Schmidt orthogonalization procedure. All electrons were included in calculations of correlation energies.

To describe the Ne−CN complex, we defined a two-dimensional Jacobi coordinate system (see Figure 1), where $R$ denotes the distance between the center of the mass of the diatomic molecule and the interacting atom. The symbol $\Theta$ represents the angle between $R$ vector and the CN bond axis ($\Theta = 0°$ corresponds to a linear Ne−CN geometry). The interatomic separation of the cyano radical in its $^2\Sigma^+$ ground state was fixed at the experimental distance of 1.17 Å.[52]

Two different basis sets were used in this study. The first, used for the C and N atoms, reported by Sadlej,[53] is the near

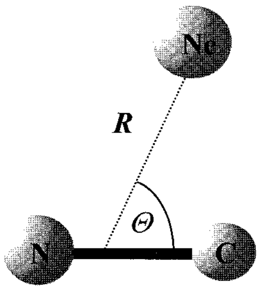

**Figure 1.** Coordinate system for the Ne−CN complex.

triple-ζ quality basis set augmented by the polarization functions optimized to reproduce the molecular electric properties, especially polarizabilities. This basis set is designated as C, N(10s6p4d/5s3p2d). The basis set employed for the Ne atom (specified as 13s8p4d2f/7s6p4d2f) is denoted as aug-cc-pCVTZ. It represents the correlation consistent core−valence basis set, which extends the ideas of the original Dunning cc-pVTZ set[54] by including extra functions designed for the core−core and core−valence correlation.[55] Pure sets of d and f functions (i.e., five d functions and seven f functions) were used in this study.

## Results and Discussion

**A. Characterization of the PES.** To acquire reliability in our results and conclusions, it is necessary to discuss the suitability of our theoretical findings. To ensure that the methods based on the single-determinant wave function are sufficient to describe the complex Ne−CN in its ground state, the CISD and MR-CI test calculations were performed for the T-shaped and linear geometries at $R = 3.7$ Å by MOLCAS-3 program package.[56] A reference space for the MR-CI calculations was generated by a subsequent extension of the reference space starting from single-reference CISD calculation, until all significant configurations were included, giving a total of eight references. In all cases the $c_1{}^2$ was larger than 0.93 for the ground state, indicating that a single-determinant wave function is adequate for this complex. However, during the employment of the single-reference unrestricted approach, the spin contamination can be the additional source of errors, which for both the open-shell monomer and dimer must be of practically the same value. Otherwise, the subtraction of the dimer and monomer energies is inconsistent. Although this condition was satisfied in all our calculations, the large spin contamination from unwanted spin states ($\hat{S}^2 \approx 1.17$)[57] complicates the situation, and the application of the projection technique is required. The features of the used basis sets have been checked on the electric and magnetic properties of the CN molecule in its $^2\Sigma^+$ ground-state electron configuration: $1\sigma^2 ...4\sigma^2\ 5\sigma^1\ 1\pi^4$. In agreement with the chemical expectation, the unpaired electron was located in the $\sigma$ orbital formed by 2s and $2p_z$ AO's of the carbon atom (the bond being along the $z$ axis). The calculated Fermi contact spin densities of 0.88 for the carbon and 0.06 for the nitrogen atom are in reasonable agreement with the measured hyperfine splitting constants of $a_C = 20.99$ mT and $a_N = -0.44$ mT, respectively.[58] The natural bond orbital analysis of the RHF wave function assigns 5.16 electrons on the C−N bonding orbitals, and the additional analysis also shows 1.98 lone pair electrons on the nitrogen atom. Our resulting dipole moment ($\mu = 2.3$ D) and polarizability tensor components ($\alpha_{xx} = 12.8$ au, $\alpha_{yy} = 12.8$ au, $\alpha_{zz} = 20.0$ au) are in perfect agreement with the calculations of Urban et al.[59] who used a very large aug-cc-pV5Z basis set, but the dramatic change of the polarity from $\mu = 2.3$D (SCF) to $\mu = 1.56$D (post-HF) indicates the inevitability of including also the correlation effects in our calculations.

The computed PES at the restricted MP2 level of the theory (see Table 1S) features a single minimum located near the T-shaped Ne−CN configuration at $\Theta = 110°$, $R = 3.7$ Å, and its well depth amounts to $-145.9\ \mu E_h$. These values are in agreement with the ab initio results of Alexander et al.[26] computed at the MR-CI level of the theory. They found a minimum for the skewed T-shaped geometry at $R = 3.7$ Å and $\Theta = 130°$ with a well depth of about $-142.6\ \mu E_h$. Our potential can be compared also with the spectroscopic measurements of Lawrence et al.[22] Their PES shows a minimum at $R \approx 3.7$ Å with the well depth of $-138 \pm 20\ \mu E_h$, which coincides with both above theoretical predictions.

The lowest calculated point at the unrestricted MP2 level of theory (see Table 2S) corresponds also to an approximate T-shaped geometry, and the interaction energy amounts to $-137.6\ \mu E_h$. This result is slightly shallower when compared to the restricted MP2 value of $-145.9\ \mu E_h$. However, the projected UMP4 computations offer the data of quality comparable with the restricted MP2 results.

To visualize the shape of the PES, in Figures 2 and 3 we demonstrate the curves representing cuts through the surface at different values of $R$ and for $\Theta$ ranging from 0° to 180°, which were obtained at the RMP2 and UMP2 level, respectively. An inspection of Figure 2 shows that the curves in the region about $R \approx 4$ Å represent the double-well potentials with rather small barriers separating the nonequivalent minima. In the region of the vdW minimum ($R = 3.7$ Å), the interaction potential as a function of $R$ and $\Theta$ is flat, and the anisotropy is relatively weak. In contrast, the anisotropy of the potential is very pronounced in the short-range region ($R \approx 3.1$ Å). The potential shows a very strong angular dependence, the interaction energy changes from 2200 $\mu E_h$ at $\Theta = 0°$ to approximately 100 $\mu E_h$ at $\Theta = 90°$, i.e., roughly by a factor of 22. Compared with the RMP2 potential, the UMP2 surface is more repulsive in the region of the minima and the double-well character of the curves appears at $R \approx 3.7$ Å. Additionally, the position of the global minimum is nearer to the C end, at the geometry with $R \approx 3.7$ Å and $\Theta = 50°$. Finally, we can conclude that the presented RMP2 PES is closer to the recently published MR-CI surface in comparison with the UMP2 potential. However, as can be seen in Figure 3, the projected UMP4 calculations (for $R = 3.7$ Å) reveal behavior similar to the RMP2 approach.

**B. Partitioning of Interaction Energies.** The next goal of this study was to investigate the physical origin of the stability in the vdW complex including the unpaired electron. Using the decomposition of the RHF and UHF supermolecular MP2 interaction energy, we tried to analyze how the fundamental components determine its anisotropy in a particular region (at $R = 3.7$ Å).

The HF interaction energies ($\Delta E^{HF}$) display a strong angular dependence with a minimum at 90° and maxima at 0° and 180°. The anisotropy of HF interaction energy is, in principle, determined by the HL interaction ($\Delta E^{HL}$) and HF deformation energies. The leading $\Delta E^{HL}$ energy is positive due to the dominant exchange-penetration energy contribution. The attractive coloumbic forces, represented by the HF electrostatic ($E_{es}^{(100)}$) term, are implicitly included in the $\Delta E^{HL}$ term.

The dependence of the selected interaction energy contributions on the Jacobi angle for a fixed value of the intermolecular separation $R$ is presented in Figures 4 and 5. It should be noted that the shape of these curves is simply a consequence of the

**TABLE 1: Interaction Energy Contributions of UHF $\Delta E^{HF}$ and $\Delta E^{(2)}$ and Supermolecular MP2−MP4 Interaction Energies (in $\mu E_h$) Obtained for Different Values of $R$ (in Å), $r$ (in Å), and $\Theta$[a]**

| | $R = 3.7, \Theta = 90°$ | | | $R = 4.1, \Theta = 180°$ | | | $R = 4.2, \Theta = 0°$ | | |
|---|---|---|---|---|---|---|---|---|---|
| energy | $r = 1.1$ | $r = 1.17$ | $r = 1.3$ | $r = 1.1$ | $r = 1.17$ | $r = 1.3$ | $r = 1.1$ | $r = 1.17$ | $r = 1.3$ |
| $E_{es}^{(100)}$ | −37.6 | −41.9 | −44.7 | −24.4 | −27.4 | −36.3 | −24.5 | −27.3 | −35.4 |
| $E_{exch}^{HL}$ | 130.4 | 142.2 | 147.5 | 106.0 | 116.0 | 145.3 | 74.5 | 83.5 | 111.4 |
| $\Delta E^{HL}$ | 92.8 | 100.3 | 102.8 | 81.6 | 88.6 | 109.0 | 50.0 | 56.2 | 76.0 |
| $E_{ind}^{(200)}$ | −47.1 | −52.6 | −55.1 | −44.3 | −45.5 | −51.8 | −34.7 | −37.3 | −42.8 |
| $\Delta E_{def}^{HF}$ | −11.3 | −11.1 | −9.4 | −21.9 | −19.9 | −17.6 | −25.2 | −25.6 | −24.7 |
| $\Delta E^{HF}$ | 81.5 | 89.2 | 93.4 | 59.7 | 68.7 | 91.4 | 24.8 | 30.6 | 51.3 |
| | (75) | (77) | (88) | (64) | (76) | (97) | (23) | (34) | (55) |
| $E_{disp}^{(200)}$ | −223.7 | −230.1 | −229.9 | −204.8 | −217.2 | −236.2 | −158.6 | −170.3 | −190.5 |
| $\Delta E^{(2)}$ | −196.7 | −187.6 | −175.2 | −177.6 | −194.6 | −215.1 | −133.1 | −150.2 | −175.8 |
| $E^{(MP2)}$ | −115.2 | −98.4 | −81.8 | −117.9 | −125.9 | −123.7 | −108.3 | −119.6 | −124.5 |
| | (−121) | (−109) | (−87) | (−114) | (−119) | (−118) | (−109) | (−116) | (−122) |
| $E^{(MP3)}$ | −104.3 | −91.3 | −79.3 | −104.8 | −110.3 | −113.8 | −95.7 | −104.1 | −112.0 |
| | (−109) | (−100) | (−85) | (−101) | (−105) | (−107) | (−95) | (−101) | (−108) |
| $E^{(MP4)}$ | −132.5 | −120.6 | −106.5 | −138.5 | −148.9 | −158.3 | −122.4 | −133.5 | −145.7 |
| | (−137) | (−130) | (−113) | (−135) | (−143) | (−152) | (−123) | (−131) | (−142) |

[a] The data in parentheses represent the projected UHF results.

**TABLE 2: Interaction Energy Contributions of RHF $\Delta E^{HF}$ and $\Delta E^{(2)}$ and Supermolecular MP2 Interaction Energies ($\mu E_h$) Obtained for Different Values of $R$ (in Å), $r$ (in Å), and $\Theta$**

| | $R = 3.7, \Theta = 90°$ | | $R = 4.1, \Theta = 180°$ | | $R = 4.2, \Theta = 0°$ | |
|---|---|---|---|---|---|---|
| energy | $r = 1.1$ | $r = 1.17$ | $r = 1.1$ | $r = 1.17$ | $r = 1.1$ | $r = 1.17$ |
| $E_{es}^{(100)}$ | −39.7 | −47.8 | −23.3 | −24.6 | −26.6 | −30.4 |
| $E_{exch}^{HL}$ | 137.2 | 159.6 | 102.2 | 106.7 | 82.5 | 94.9 |
| $\Delta E^{HL}$ | 97.5 | 111.8 | 78.9 | 82.1 | 55.9 | 64.5 |
| $E_{ind}^{(200)}$ | −51.2 | −63.1 | −42.6 | −40.9 | −43.6 | −49.4 |
| $\Delta E_{def}^{HF}$ | −12.6 | −15.0 | −21.4 | −18.6 | −26.7 | −29.7 |
| $\Delta E^{HF}$ | 84.9 | 96.8 | 57.5 | 63.5 | 29.2 | 34.8 |
| $E_{disp}^{(200)}$ | −236.3 | −252.9 | −210.9 | −230.9 | −180.3 | −202.0 |
| $\Delta E^{(2)}$ | −220.2 | −237.5 | −176.7 | −195.1 | −142.7 | −150.1 |
| $E^{(MP2)}$ | −135.3 | −140.7 | −119.1 | −131.6 | −113.5 | −115.3 |

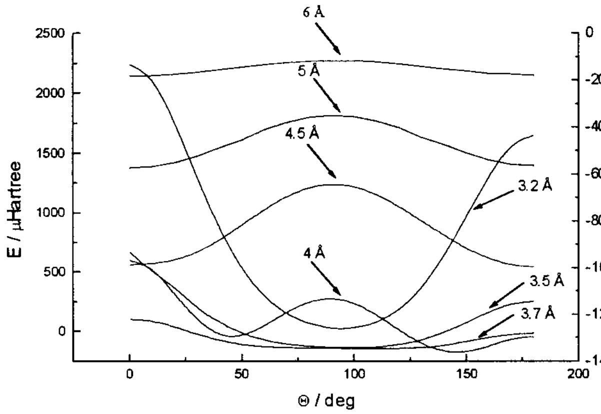

**Figure 2.** Angular dependence of the supermolecular interaction energy, obtained through the second-order of the restricted MP2 theory. (The arrows oriented from left to right stand for right axes and vice versa.)

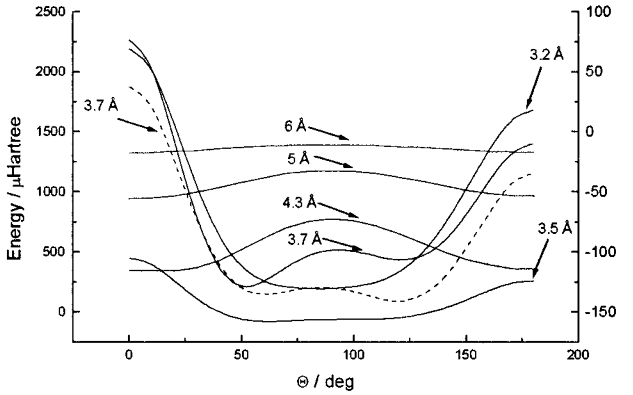

**Figure 3.** Angular dependence of the interaction energy, obtained through the second-order of the unrestricted MP2 (solid) and the fourth-order projected MP4 (dashed) theory. (The arrows oriented from left to right stand for right axes and vice versa.)

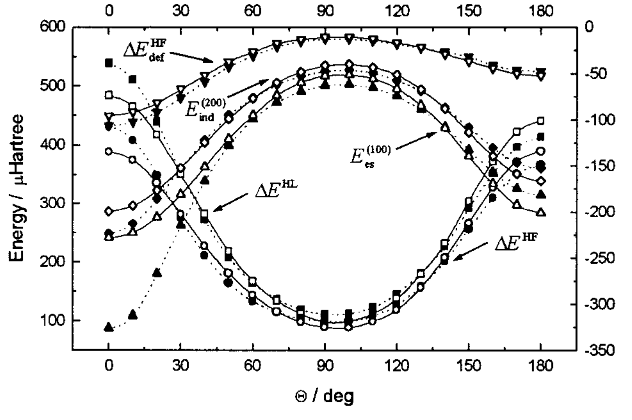

**Figure 4.** Angular dependence of the $\Delta E^{HF}$ energy and its components at $R = 3.7$ Å: (solid symbols) RHF; (open symbols) UHF. (The arrows oriented from left to right stand for right axes and vice versa.)

used coordinate system. With $R$ fixed at 3.7 Å, the Ne atom is much closer to the carbon atom at $\Theta = 0°$ or to the nitrogen atom at $\Theta = 180°$ than it is to either atom at 90°. This geometry effect readily explains the increase of the exchange repulsion and dispersion interactions for the linear geometries. Consequently, if the distance between interacting atoms decreases, repulsive exchange-penetration contributions predominate over the attractive HF electrostatic and HF dispersion energies.

The HF deformation term ($\Delta E_{def}^{HF}$) shows an approximately reciprocal character to the HL anisotropy and has a nominal smoothing effect on the total SCF interaction energy around the linear configurations. Although the CN radical system has the permanent dipole moment ($\mu$ = 1.5D), the second-order induction energies ($E_{ind}^{(200)}$) do not provide a good approximation of the $\Delta E_{def}^{HF}$ energy due to the exchange-repulsion induction effects (compare the differences between $\Delta E_{def}^{HF}$ and $E_{ind}^{(200)}$ energies in Figure 4). Both mentioned terms have the smallest values around the perpendicular geometry and therefore $\Delta E^{HF}$

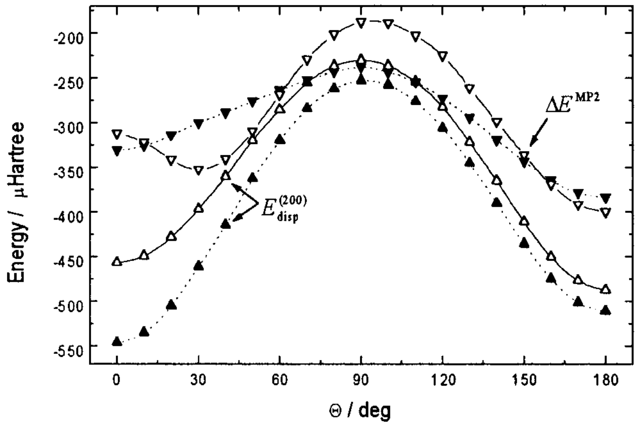

**Figure 5.** Angular dependence of the $\Delta E^{(2)}$ energy and its dispersion components $E^{(200)}_{\rm disp}$ at $R = 3.7$ Å: (solid symbols) RHF; (open symbols) UHF.

energies are very close to the sum of the electrostatic and exchange components, $\Delta E^{\rm HL}$.

Similarly, $\Delta E^{(2)}$ plays an important role in forming the shape of the total RHF and UHF MBPT2 interaction energies (Figure 5). One can see that $E^{(200)}_{\rm disp}$ is the dominant attractive contribution. It favors the linear orientations whereas the *T* minimum occurs at the lowest value of $-230$ $\mu E_{\rm h}$ (UHF) and $-253$ $\mu E_{\rm h}$ (RHF), respectively. The positive values obtained from the difference of the $\Delta E^{(2)}$ and the above-mentioned dispersion terms in both structures indicate the nonnegligible role of the remaining exchange-dispersion, correlation-electrostatic as well as deformation energies.

**C. Effect of CN Bond Length on the Interaction Energy.** The origin of the minima for the linear forms (Ne···N, Ne···C) as well as the influence of the intramolecular CN bond distance (*r*) on the interaction energy is also quite interesting. Unfortunately, with increasing CN bond length ($r > 1.25$ Å) the energy gap between the X $^2\Sigma$ and A $^2\Pi$ states of cyano radical diminishes.[57] This fact not only can cause the SCF procedure to fail to converge but also may cause it to converge to a different state than has been initially intended. To avoid these problems, the stability of SCF wave functions was tested using the single-excitation configuration interaction.[60] Although the UHF wave functions were found to be stable with respect to the perturbation from the excited configurations, the convergence of the RHF wave functions was highly oscillating. Therefore, the effect of the CN bond elongation on the interaction energy was studied within the UHF approximation only.

When the CN bond is elongated to 1.30 Å, the interaction energies reveal the greater stability for the linear configurations. On the other hand, when *r* is shortened to 1.10 Å, the energy of the T-shaped structure is found to be lower than the energy in the approximate equilibrium bond of 1.17 Å (cf. Tables 1 and 2). The results of the supermolecular UHF calculations up to the fourth-order MBPT level indicate that the T-shaped structure is not so sensitive to the changes of *r* as the linear configurations. We found the similar *r* dependence for both the spin-contaminated and the projected UHF calculations (see Table 1).

The selected UHF interaction energy components depend on the changes of the CN bond length mainly in the linear configurations. Evidently, the induction and dispersion energies play an important role in strengthening the interaction energy. The exchange-penetration effects in $\Delta E^{(2)}$ seem to be less important than the in the $\Delta E^{\rm HF}$ energies (cf. $\Delta E^{\rm HL}$, $\Delta E^{\rm HF}_{\rm def} - E^{(200)}_{\rm ind}$, and $\Delta E^{(2)} - E^{(200)}_{\rm disp}$ in Table 1.)

**TABLE 3: Equilibrium Distances $R$ (in Å), Dissociation Energies $D_e$ (in cm$^{-1}$), Ground-Vibrational-State Dissociation Energies $D_0$ (in cm$^{-1}$), and Harmonic Stretching ($\omega_{\rm stre}$) and Bending ($\omega_{\rm bend}$) Frequencies (in cm$^{-1}$) for the Complex Ne($^1$S)−CN($^2\Sigma^+$)**

| method | $R$ | Θ | $\omega_{\rm stre}$ | $\omega_{\rm bend}$ | $D_e$[a] | $D_0$[a] |
|---|---|---|---|---|---|---|
| RMP2 | 3.69 | 103° | 16.2 | 5.9 | 32.01 | 20.96[b] |
| UMP2 | 3.82 | 47° | 14.9 | 7.7 | 30.20 | 18.90[b] |

[a] Conversion factor: 1 cm$^{-1}$ = 4.556$\mu E_{\rm h}$. [b] $D_0 = D_{\rm c} - {}^1/_2(\omega_{\rm stre} + \omega_{\rm bend})$.

**D. Vibrational Analysis.** The good description attained for the structure and energetics of the Ne−CN complex within the supermolecular MP2 approach stimulated us to analyze the vibrational spectrum for the intermolecular degrees of freedom. Although the experimental ro-vibrational spectrum for the Ne−CN complex was not detected up to the present time, Lawrence et al.[22] found hot band in the electronic spectrum of this system originating from the low-lying level. As interpretation of these spectra may be difficult, creation of the PES's should be helpful for their assignment. Another motivation is to answer the question how the vibrational spectrum of the complex may influence the topology of the PES.

To accomplish the vibrational analysis, the calculated ab initio points were fitted to the analytical surface by the cubic spline method implemented in the SURVIB program package.[61] The harmonic frequencies were found by evaluating the second derivatives at the appropriate minima and diagonalizing the mass-weighted Cartesian force constant matrix. The results of these calculations are summarized in Table 3. The obtained values clearly show the distinctly different topologies of the calculated RMP2 and UMP2 PES's. The smaller stretching frequency for the UMP2 surface is the consequence of the shallower radial cuts in the vicinity of the vdW minimum with respect to the RMP2 potential. Similarly, the sharper angular cuts cause the increasing bending frequency based on the UMP2 PES in comparison with its counterpart calculated from RMP2 surface. Although, the depths of the wells are also significantly influenced, the zero-point energies are about one-third of the dissociation energies, the ZPE corrections keep the difference between RMP2 and UMP2 well depths roughly at the same level.

However, it should be added that our harmonic vibrational analysis represents a crude approximation. The main discrepancy arises from the shallowness of the PES, since the large amplitude motions of the Ne atom are likely to be highly anharmonic. Furthermore, the barriers to the linearity are 3.5 and 5.0 cm$^{-1}$, for the C and N ends, respectively. Thus, the complex can be very close to a free rotor and probably the angular momentum of the cyano radical is quenched by the presence of the Ne atom only very weakly.

The vibrational frequencies of the intermolecular stretching and bending motions should be calculated with more sophisticated models based on the solution of the ro-vibrational Hamiltonian. Such betterments would tend to improve the values of the vibrational frequencies, and this would lead to a more reliable description of the surface.

## Summary

The interaction potential energy surface of the Ne−CN(X $^2\Sigma^+$) van der Waals complex has been investigated in a broad range of geometries using the supermolecular approach based on the RHF as well as UHF wave function. A way of the interaction energy decomposition applicable to open-shell systems was proposed. This scheme was used to analyze the origins of the interaction for the studied system. As was shown, the dominant attraction part of the interaction energy comes mainly from the dispersion and induction contributions. The PES was found to be weakly anisotropic in the region of the vdW minimum. On the contrary, the ab initio potential indicates a very pronounced anisotropy in the repulsive region. To estimate the influence of the zero-point correction on the stability of the complex under study, some harmonic vibrational properties were evaluated from the presented PES calculations.

It is necessary to emphasize that the more appropriate comprehension of the processes connected with spectral and scattering measurements demands a more complex description of the PES in relation to the excited states. Despite the natural difficulties of the supermolecular and I-PT approach based on the single-determinant RHF as well as the UHF wave function, it could be a useful tool to perform theoretical studies of the open-shell vdW systems. Works of this type are likely to intensify soon.

**Acknowledgment.** We are grateful to our colleague, Dr. M. Breza, for helpful discussions and encouragement. We thank reviewers for suggestions leading to an improvement of our manuscript. The work reported in this paper has been funded by the Slovak Grant Agency, projects no. 1/4205/97 and 1/4199/97.

## References and Notes

(1) Leopold, K. R.; Fraser, G. T.; Novick S. E.; Klemperer, W. *Chem. Rev.* **1994**, *94*, 1807.

(2) Nesbitt, D. J. *Annu. Rev. Phys. Chem.* **1994**, *45*, 367.

(3) Cohen, R. C.; Saykally, R. J. *J. Phys. Chem.* **1992**, *96*, 1024.

(4) Hutson, J. M. *Annu. Rev. Phys. Chem.* **1990**, *41*, 123.

(5) Bacic, Z.; Miller, R. E. *J. Phys. Chem.* **1996**, *100*, 12945.

(6) Furio, N.; Ali, A.; Dagdigian, P. J. *Chem. Phys. Lett.* **1986**, *125*, 561.

(7) Furio, N.; Ali, A.; Dagdigian, P. J. *J. Chem. Phys.* **1986**, *85*, 3860.

(8) Jihua, G.; Ali, A.; Dagdigian, P. J. *J. Chem. Phys.* **1986**, *85*, 7098.

(9) Ali, A.; Jihua, G.; Dagdigian, P. J. *J. Chem. Phys.* **1987**, *87*, 2045.

(10) Randall, R. W.; Chuang, C.-C.; Lester, M. J. *Chem. Phys. Lett.* **1992**, *200*, 113.

(11) Heaven, M. C. *Annu. Rev. Phys. Chem.* **1992**, *42*, 283.

(12) Heaven, M. C. *J. Chem. Phys.* **1993**, *97*, 8567.

(13) Qian, H.-B.; Seccombe, D.; Howard, B. J. *J. Chem. Phys.* **1997**, *107*, 7658.

(14) Qian, H.-B.; Low, S. J.; Seccombe, D.; Howard, B. J. *J. Chem. Phys.* **1997**, *107*, 7651.

(15) Meyer, H. *J. Chem. Phys.* **1997**, *107*, 7732.

(16) Carter, C. C.; Miller, T. A. *J. Chem. Phys.* **1997**, *107*, 3447.

(17) Mulliken, R. S. *J. Chim. Phys.* **1964**, *61*, 20.

(18) Lin, Y.; Heaven, M. C. *J. Chem. Phys.* **1991**, *64*, 5765.

(19) Bondybey, V. E. *J. Chem. Phys.* **1977**, *66*, 995.

(20) Katayama, P. H.; Miller, T. A.; Bondybey, V. E. *J. Chem. Phys.* **1979**, *71*, 1662.

(21) Halpern, J. B.; Huong, Y.; Titauchuk, T. *Astrophys. Space Sci.* **1996**, *236*, 11.

(22) Lawrence, W. G.; Chen, Y.; Heaven, C. M. *J. Chem. Phys.* **1997**, *107*, 7163.

(23) Alexander, M. H.; Corey, G. C. *J. Chem. Phys.* **1986**, *84*, 100.

(24) Werner, H. J.; Follmeg, B.; Alexander, M. H. *J. Chem. Phys.* **1988**, *89*, 3139.

(25) Werner, H. J.; Follmeg, B.; Alexander, M. H.; Lemoine, D. *J. Chem. Phys.* **1989**, *91*, 5142.

(26) Yang, M.; Alexander, M. H. *J. Chem. Phys.* **1997**, *107*, 7148.

(27) Mayer, W. *Int. J. Quantum. Chem. Symp.* **1971**, *5*, 341.

(28) Mayer, W. *Theor. Chim. Acta* **1974**, *35*, 277.

(29) Werner, H.-J.; Reinsch, E. A. *Advanced Theory and Computational Approaches to the Electronic Structure of Molecules*; Dykstra, C. E., Ed.; Reidel: Dordrecht, The Netherlands, 1984; p 79.

(30) Lee, E. P. F.; Wright, T. G. *J. Chem. Phys.* **1998**, *109*, 157.

(31) Chalasinski, G.; Szczesniak, M. M. *Chem. Rev.* **1994**, *94*, 1723 and references therein.

(32) Chalasinski, G.; Simons, J. *Chem. Phys. Lett.* **1988**, *148*, 289.

(33) Chalasinski, G.; Gutowski, M.; Szczesniak, M. M.; Sadlej, A.; Scheiner, S. *J. Chem. Phys.* **1994**, *101*, 6800.

(34) Cybulski, S. M.; Burcl, R.; Chalasinski, G.; Szczesniak, M. M. *J. Chem. Phys.* **1995**, *103*, 10116.

(35) Cybulski, S. M.; Burcl, R.; Chalasinski, G.; Szczesniak, M. M. *J. Chem. Phys.* **1996**, *104*, 7997.

(36) Kendal, R. A.; Chalasinski, G.; Klos, J.; Bukowski, R.; Severson, M. W.; Szczesniak, M. M.; Cybulski, S. M. *J. Chem. Phys.* **1998**, *108*, 3235.

(37) Cybulski, S. M.; Chalasinski, G.; Szczesniak, M. M. *J. Chem. Phys.* **1996**, *105*, 9525.

(38) Burcl, R.; Krems, R. V.; Buchachenko, A. A.; Szczesniak, M. M.; Chalasinski, G.; Cybulski, S. M. *J. Chem. Phys.* **1998**, *109*, 2144.

(39) Kvasnička, V.; Laurinc, V.; Biskupič, S. *Mol. Phys.* **1981**, *42*, 1345.

(40) Čársky, P.; Zahradník, R.; Hubač, I.; Urban, M.; Kellö V. *Theor. Chim. Acta* **1980**, *56*, 315.

(41) Lukeš, V.; Laurinc, V.; Biskupič, S. *J. Comput. Chem.* **1999**, *20*, 857.

(42) Bussery, B.; Wormer, P. E. S. *J. Chem. Phys.* **1993**, *99*, 1230.

(43) Rybak, S.; Jeziorski, B.; Szalewicz, K.; *J. Chem. Phys.* **1991**, *95*, 6576 and references therein.

(44) Surján, P. R.; del Valle, C. P. *Theor. Chim. Acta* **1996**, *94*, 333 and references therien.

(45) Laurinc, V.; Lukeš, V.; Biskupič, S. *Theor. Chem. Acc.* **1998**, *99*, 53 and references therein.

(46) Löwdin, P.-O. *Adv. Phys.* **1956**, *5*, 1.

(47) Jeziorski, B.; van Hemert N. C. *Mol. Phys.* **1976**, *31*, 713.

(48) Salter, E. A.; Trucks, G. W.; Bartlett, R. J. *J. Chem. Phys.* **1989**, *90*, 1752 and references therein.

(49) Cybulski, S. M. *J. Chem. Phys.* **1992**, *97*, 7545 and references therein.

(50) Frisch, M. J.; Trucks, G. W.; Schlegel, H. B.; Gill, P. M. W.; Johnson, B. G.; Robb, M. A.; Cheeseman, J. R.; Keith, T.; Petersson, G. A.; Montgomery, J. A.; Raghavachari, K.; Al-Laham, M. A.; Zakrzewski, V. G.; Ortiz, J. V.; Foresman, J. B.; Cioslowski, J.; Stefanov, B. B.; Nanayakkara, A.; Challacombe, M.; Peng, C. Y.; Ayala, P. Y.; Chen, W.; Wong, M. W.; Andres, J. L.; Replogle, E. S.; Gomperts, R.; Martin, R. L.; Fox, D. J.; Binkley, J. S.; Defrees, D. J.; Baker, J.; Stewart, J. P.; Head-Gordon, M.; Gonzalez, C.; Pople, J. A. *Gaussian 94*; Gaussian, Inc.: Pittsburgh, PA, 1994.

(51) Boys, S. F.; Bernardi, F. *Mol. Phys.* **1970**, *19*, 553.

(52) Huber, K. P.; Herzberg, G. *Molecular Spectra and Molecular Structure IV. Constants of Diatomic Molecules*; Van Nostrand Reinhold: New York, 1979.

(53) Sadlej, A. J. *Collect. Czech. Chem. Commun.* **1988**, *53*, 1995.

(54) Kendall, R. A.; Dunning, T. H., Jr.; Harrison, R. J. *J. Chem. Phys.* **1992**, *96*, 6796.

(55) Basis sets were obtained from the Extensible Computational Chemistry Environment Basis Set Database, version 1.0. Feller, D.; Schuchardt, K. Pacific Northwest Laboratory: P.O. Box 999, Richland, WA 99352.

(56) Anderson, K.; Blomberg, M. R. A.; Fülscher, M. P.; Karlström, G.; Kellö, V.; Lindh, R.; Malmqvist, P-Å; Noga, J.; Olsen, J.; Roos, B. O.; Sadlej, A. J.; Siegbahn, P. E. M.; Urban, M.; Widmark, P.-O. *Molcas-3*; University of Lund: Lund, Sweden 1994.

(57) Lauderdale, W. J.; Stanton, J. F.; Gauss, J.; Watts, J. D.; Bartlett, R. J. *Chem. Phys. Lett.* **1991**, *187*, 21.

(58) Landolt-Börnstein. *Magnetic properties of free radicals*; Springer-Verlag: Berlin, 1975; Vol. 9, II/9a.

(59) Urban, M.; Neogrady, P.; Raab. J.; Diercksen, G. H. F. *Collect. Czech. Chem. Commun.* **1998**, *63*, 1409.

(60) Seeger, S.; Pople, J. A. *J. Chem. Phys.* **1977**, *66*, 3045.

(61) Harding, L. B.; Ermler, W. C. *J. Comput. Chem.* **1985**, *6*, 13.